

三维配位聚合物 $[\text{C}_4\text{H}_{12}\text{N}_2]_3[\text{PMo}_{12}\text{O}_{40}]$ 的合成、结构及其电化学性质

齐艳娟* 苑晓冬 田 利

(长春师范学院化学学院, 长春 130032)

关键词: 水热合成; 哌嗪; 电化学性质

中图分类号: O614.61*2

文献标识码: A

文章编号: 1001-4861(2009)06-1110-05

Synthesis, Structure and Electrochemical Properties of Three-Dimensional Complex $[\text{C}_4\text{H}_{12}\text{N}_2]_3[\text{PMo}_{12}\text{O}_{40}]$

QI Yan-Juan* YUAN Xiao-Dong TIAN Li

(Department of Chemistry of Changchun Normal University, Changchun 130032)

Abstract: The title compound $[\text{C}_4\text{H}_{12}\text{N}_2]_3[\text{PMo}_{12}\text{O}_{40}]$ was synthesized from the hydrothermal reaction and characterized by IR, elemental analysis and X-ray signal crystal structural analysis. The crystal of the title complex belongs to trigonal space group $R\bar{3}c$ with $a=1.788\ 62\ \text{nm}$, $c=2.354\ 3\ \text{nm}$, and $V=6.522\ 62\ \text{nm}^3$, $Z=6$, $R_1=0.038\ 4$, $wR_2=0.102\ 0$. The compound consisted of piperazine and $\text{PMo}_{12}\text{O}_{40}^{3-}$, and the structure is extended to three dimensional framework owing to the hydrogen bond between the O atoms and N atoms. The bulk-modified carbon paste electrode (APM-CPE) using this compound as modifier shows a good electrocatalytic activity toward the oxidation of ascorbic acid(AA). CCDC: 707968.

Key words: hydrothermal synthesis; piperazine; electrochemical properties

The construction of supramolecular assemblies from organic or inorganic molecular building blocks has been attracting extensive interest in recent years owing to their novel and diverse topologies and potential applications in host-guest chemistry, shape-selective catalysis, absorption, electrical-conductive, magnetic, and photosensitive materials^[1-6]. Huge structures of these materials were reported, showing various architectures with 1D, 2D and 3D connections between inorganic-organic species^[7-9]. For such rational design, hydrogen bonding of conventional $\text{OH}\cdots\text{N}$ and $\text{NH}\cdots\text{O}$ motifs has been the most commonly used as supramolecular cement, yet weaker forces such as $\text{CH}\cdots\text{O}$, $\text{CH}\cdots$

N , $\text{CH}\cdots\text{I}$, or even $\text{C}\cdots\text{H}$ and $\text{C}\cdots\text{C}$ have been used^[10-12]. The organic components have been presented as charge-compensating cations such as $[\text{H}_3\text{N}(\text{CH}_2)_6\text{NH}_3][\text{Mo}_4\text{O}_{13}]^{[13]}$, $[\text{HN}(\text{C}_2\text{H}_4)_3\text{NH}][\text{V}_6\text{O}_{14}]\cdot\text{H}_2\text{O}^{[14]}$, $[\text{V}_4\text{O}_{10}(\text{phen})_2]^{[15]}$, $[\text{MoO}_3(2,2'\text{-bpy})]$ (bpy=bipyridine)^[16], $[\text{MoO}_3(4,4'\text{-bpy})_{0.5}]^{[17]}$. Typically, the P-Mo system possesses specialty in constructing the novel inorganic-organic channel structure material, which extremely rich the classics POMs chemistry. Such as $[(\text{CH}_2\text{OH})_3\text{CNH}_3]_3\text{PMo}_{12}\text{O}_{40}\cdot 5\text{H}_2\text{O}^{[18]}$, $(\text{N}(\text{C}_4\text{H}_9)_4)_2\text{H}_9[\{(\text{P}_2\text{O}_7)\text{Mo}_{15}\text{O}_{45}\}_2][\text{PMo}_{12}\text{O}_{40}]^{[19]}$ and $[\{\text{Na}(\text{dibenzo-18-crown-6})-(\text{MeCN})\}_3\{\text{PMo}_{12}\text{O}_{40}\}]^{[20]}$.

Here we report the preparations and crystal structure characterizations and electrical property of the

收稿日期: 2008-12-02。收修改稿日期: 2009-03-31。

吉林省科技发展计划项目资助(No.20071163)。

*通讯联系人。E-mail: qiyajuan@163.com; Tel: 0431-86168093

第一作者: 齐艳娟, 女, 43 岁, 博士, 教授; 研究方向, 配位化学。

title compound [C₄H₁₂N₂]₃[PMo₁₂O₄₀].

1 Experimental

1.1 General procedures

All reagents were purchased commercially and used without further purification. Deionized water was used for the hydrothermal synthesis. The hydrothermal reaction was performed in a 15 mL Teflon-lined stainless steel autoclave at 180 °C under autogenous pressure. Elemental analyses (C, H and N) were performed on a Perkin-Elmer 2400 CHN Elemental Analyzer. Mo element is determined by ICP-AES analysis. The infrared spectra were recorded on an Alpha Centaur FTIR spectrometer with pressed KBr pellets in the 4 000~500 cm⁻¹ region. Electrochemical experiments were performed with a CHI 660 A (CH instruments, USA) Electrochemical Analyzer. Quantitative estimation of iodate in salt samples was detected with a Model Shimadzu UV-3100 spectrophotometer.

1.2 Preparation of [C₄H₁₂N₂]₃[PMo₁₂O₄₀]

A mixture of Na₂MoO₄·2H₂O, H₃PO₄ and piperazine in the mole ratio 7.5:0.1:1 was adjusted to pH=3.5

by addition of HCl and heated at 180 °C for 5 d, black crystals were isolated (41% yield on Mo). Calcd. for C₁₂H₃₆Mo₁₂N₆O₄₁P(%): C, 6.9; H, 1.7; P, 1.5; Mo, 54.8; found(%): C, 7.1; H, 1.8; P, 1.4; Mo, 54.2. IR: 803, 880, 957, 1 062, 1 210, 1 318, 1 385, 1 445, 1 536 cm⁻¹.

1.3 X-ray crystal structure determination

The diffraction data collection of the title compound with dimensions 0.45 mm×0.36 mm×0.26 mm was performed at 293 K on Siemens P4 four-circle diffractometer with Mo K α radiation (λ =0.071 073 nm) and the ω scan mode in the range of 2.28°< θ <26.00°. An empirical absorption correction on the data was applied. The structure was solved by direct methods with SHELXS-97 program and refined by a full-matrix least-squares technique based on F^2 using the SHELXL-97 program. All of the nonhydrogen atoms were refined anisotropically. All hydrogen atoms were treated as riding on their attached atoms. Crystallographic data for the structure of the title compound are summarized in Table 1. Selected bond lengths and angles are given in Table 2.

CCDC: 707968.

Table 1 Crystal data and structure refinement for [C₄H₁₂N₂]₃[PMo₁₂O₄₀]

Empirical formula	C ₁₂ H ₃₆ Mo ₁₂ N ₆ O ₄₁ P	Crystal size / mm	0.31×0.15×0.11
Temperature / K	293(2)	θ range for data collection / (°)	2.28~26.00
Space group	$R\bar{3}c$	Limiting indices	$-22 \leq h \leq 21, -19 \leq k \leq 22, -28 \leq l \leq 22$
Crystal system	Trigonal	Reflections collected	11 499
a / nm	1.788 62(8)	Independent reflections (R_{int})	1 420 (0.038 0)
c / nm	2.354 3(2)	Independent reflections [$I > 2\sigma(I)$]	1 402
Volume / nm ³	6.522 72(70)	Data / restraints / parameters	1 402 / 0 / 144
Z	6	Goodness-of-fit on F^2	1.158
Absorption coefficient / mm ⁻¹	3.497	Final R indices [$I > 2\sigma(I)$]	$R_1=0.038\ 4, wR_2=0.102\ 0$
$F(000)$	5 982		

Table 2 Selected bond lengths (nm) and bond angles (°)

Mo(1)-O(4)#1	0.196 5(5)	P(1)-O(2)#5	0.154 8(7)	O(3)-O(2)#3	0.174 9(10)
Mo(1)-O(2)#1	0.248 4(7)	P(1)-O(2)#1	0.154 8(7)	O(3)-O(2)#1	0.174 9(10)
Mo(2)-O(7)#2	0.191 6(5)	O(2)-O(3)#3	0.174 9(10)	O(3)-Mo(2)#5	0.248 3(7)
Mo(2)-O(2)#1	0.244 1(7)	O(2)-O(2)#1	0.179 4(10)	O(3)-Mo(2)#2	0.248 3(7)
Mo(2)-O(5)#1	0.193 7(5)	O(2)-O(2)#4	0.179 4(10)	O(4)-Mo(1)#4	0.196 5(5)
P(1)-O(3)#3	0.149 2(13)	O(2)-Mo(2)#4	0.244 1(7)	O(5)-Mo(2)#4	0.193 7(5)
P(1)-O(2)#4	0.154 8(7)	O(2)-Mo(1)#4	0.248 4(7)	O(7)-Mo(2)#5	0.191 6(5)
P(1)-O(2)#2	0.154 8(7)	O(2)-O(3)#4	0.174 9(10)	N(1)-C(1)#6	0.147 9(8)
P(1)-O(2)#3	0.154 8(7)	O(3)-O(2)#4	0.174 9(10)		

Continued Table 2

O(6)-Mo(1)-O(4)#1	100.9(3)	O(6)-Mo(1)-O(1)	100.7(3)	O(5)-Mo(1)-O(4)#1	85.7(3)
O(6)-Mo(1)-O(1)	156.9(4)	O(6)-Mo(1)-O(2)	160.5(3)	O(4)-Mo(1)-O(4)#1	156.8(5)
O(5)-Mo(1)-O(2)	65.7(3)	O(1)-Mo(1)-O(4)#1	84.7(2)	O(4)#1-Mo(1)-O(2)	93.1(3)
O(4)-Mo(1)-O(2)	64.9(3)	O(4)-Mo(1)-O(2)#1	94.0(3)	O(1)-Mo(1)-O(2)	93.9(3)
O(1)-Mo(1)-O(2)#1	63.0(3)	O(6)-Mo(1)-O(2)#1	157.0(3)	O(2)-Mo(1)-O(2)#1	42.5(2)
O(5)-Mo(1)-O(2)#1	93.9(3)	O(8)-Mo(2)-O(1)	101.7(4)	O(4)#1-Mo(1)-O(2)#1	63.2(3)
O(8)-Mo(2)-O(7)#2	101.2(3)	O(8)-Mo(2)-O(7)	100.9(3)	O(1)-Mo(2)-O(7)#2	157.1(4)
O(7)-Mo(2)-O(1)	88.9(3)	O(7)-Mo(2)-O(5)#1	157.7(3)	O(7)-Mo(2)-O(7)#2	88.4(3)
O(7)#2-Mo(2)-O(5)#1	84.9(3)	O(8)-Mo(2)-O(5)#1	101.2(3)	O(7)-Mo(2)-O(2)#1	93.6(3)
O(1)-Mo(2)-O(5)#1	89.1(2)	O(7)#2-Mo(2)-O(2)#1	93.2(3)	O(8)-Mo(2)-O(2)#1	159.7(3)
O(8)-Mo(2)-O(3)	158.7(4)	O(1)-Mo(2)-O(2)#1	64.3(3)	O(1)-Mo(2)-O(3)	94.1(3)
O(5)#1-Mo(2)-O(2)#1	65.7(3)	O(5)#1-Mo(2)-O(3)	93.3(3)	O(7)-Mo(2)-O(3)	64.7(3)
O(2)#1-Mo(2)-O(3)	41.6(3)	O(7)#2-Mo(2)-O(3)	64.3(3)		

Symmetry transformations used to generate equivalent atoms: #1: $y, -x+y+1, -z$; #2: $-x+y+1, -x+2, -z$; #3: $-x+2, -y+2, -z$;

#4: $x-y+1, x, -z$; #5: $-y+2, x-y+1, z$; #6: $-x+1, -y+1, -z$.

1.4 Preparation of the bulk-modified carbon paste electrode (APM-CPE)

Preparation of the electrode was performed by mixing 40 mg of carbon powder with 200 mg of graphite and paraffin in varying proportions. The components were blended to obtain a homogeneous paste. Subsequently, 300 mg of the initial paste was mixed with 130 mg of $[C_4H_{12}N_2]_3[PMo_{12}O_{40}]$. This carbon paste was packed into the glass tube with $\Phi=3$ mm in which a wire was wound to produce the electrical contact. The face was polished with weighing paper. Freshly prepared carbon paste electrodes were stored in a fume hood prior to measurement. The bare electrode can be prepared in the same process as above with no $[C_4H_{12}N_2]_3[PMo_{12}O_{40}]$. Freshly prepared carbon paste electrodes were stored in a fume hood prior to measurement.

2 Results and discussion

2.1 Crystal structure

As shown in Fig.1, the compound consisted of piperazine and $PMo_{12}O_{40}^{3-}$. The $PMo_{12}O_{40}$ anion shows the same type of crystallographic disorder as has been found in many crystal structures with kegggin anions^[21-24]. P-O bonds range from 0.149 3(12)~0.154 7(8) nm (mean 0.152 9 nm). The Mo-O_t (terminal) bonds are in the usual range of 0.164 1(5)~0.166 6(4) nm (mean 0.165 4 nm). The Mo-O(P) bonds are in the range of 0.246 7(7)~0.248 4 (4) nm (mean 0.248 0 nm). All Mo-Mo distan-

ces are nearly equal, ranging from 0.355 53(11)~0.356 96(10) nm (mean 0.356 27 nm). The alternating long and short Mo-O (Mo) bonds in all MoO_6 octahedra fall into two well-resolved categories: the long pairs of Mo-Ob (bridge) bonds in the range of 0.191 6(7)~0.196 6(6) nm (mean 0.193 4 nm), and the short pairs of Mo-Ob bonds in the range of 0.184 2(1)~0.188 8(6) nm (mean 0.187 5 nm).

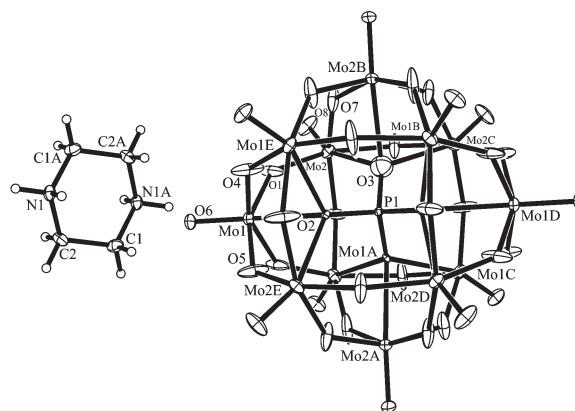


Fig.1 Structure of the title compound $[C_4H_{12}N_2]_3[PMo_{12}O_{40}]$

In the crystal, polyoxometalates and piperazine are discrete but their arrangement are not disorder. Each kegggin anion occupies three piperazine. It is also striking to note that H atom connected N atom of piperazine formed strong hydrogen bonding interactions with terminal oxygen atom ($O(6) \cdots H(1A)$ 0.211 nm) and bridge oxygen atom ($O(1) \cdots H(1A)$ 0.233 nm) of Keggin polyoxoanion, and another H atom connected N atom of

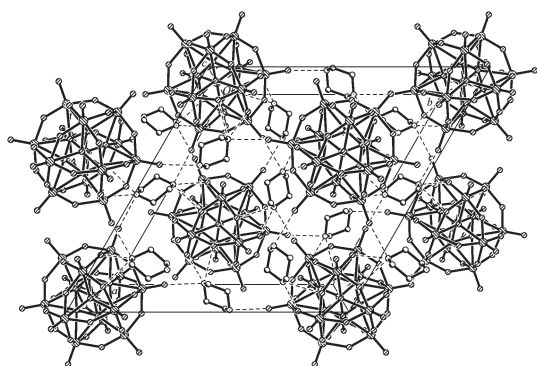
pipazine molecule formed strong hydrogen bonding interactions with two bridge oxygen atom ($\text{O}(5)\cdots\text{H}(1\text{B})$ 0.220 nm and $\text{O}(7)\cdots\text{H}(1\text{B})$ 0.222 nm) of Keggin polyoxoanion. There by extending the 1D chains into

2D layers (Table 3). These layers are further connected by short contacts into 3D supramolecular framework (Fig.2).

Table 3 Hydrogen bonds for the compound

D-H \cdots A	$d(\text{D-H})$ / nm	$d(\text{H}\cdots\text{A})$ / nm	$d(\text{D}\cdots\text{A})$ / nm	$\angle(\text{DHA}) / (^\circ)$
N(1)-H(1A) \cdots O(1)#7	0.090	0.233	0.288 5(8)	120
N(1)-H(1A) \cdots O(6)#6	0.090	0.220	0.288 3(7)	144
N(1)-H(1B) \cdots O(5)#8	0.090	0.211	0.306 3(8)	160
N(1)-H(1B) \cdots O(7)#7	0.090	0.222	0.282 6(8)	124

Symmetry transformations used to generate equivalent atoms: #1: $y, -x+y+1, -z$; #2: $-x+y+1, -x+2, z$; #3: $-x+2, -y+2, -z$; #4: $x-y+1, x, -z$; #5: $-y+2, x-y+1, z$; #6: $-x+1, -y+1, -x$; #7: $x-1/3, x-y+1/3, z-1/6$; #8: $x-y+2/3, -y+4/3, -z-1/6$.



Broken line represent hydrogen bond

Fig.2 Packing diagram of $[\text{C}_4\text{H}_{12}\text{N}_2][\text{PMo}_{12}\text{O}_{40}]$ along the c -axis

2.2 Electrochemical behavior of APM-CPE in 1.0 mol·L⁻¹ H₂SO₄

The experiments were done in a conventional three-electrode cell at room temperature. The working electrode (WE) was a modified carbon paste electrode. A platinum electrode was used as the counter electrode (CE) and a standard Ag/AgCl electrode (saturated KCl) as the reference electrode (RE). The voltammetric experiments were performed in the deoxygenated 1.0 mol·L⁻¹ H₂SO₄ solutions under nitrogen atmosphere.

The electrochemical behavior for APM-CPE in 1.0 mol·L⁻¹ H₂SO₄ solution exhibits three redox peaks. In the potential range of +800~-200 mV, no redox peaks are observed on the bare electrode shown in Fig.3a, whereas three quasi-reversible peaks with formal potential ($E_{1/2} = (E_{pa} + E_{pc})/2$) of 400, 248 and 5 mV appeared at the APM-CPE. The peak separations (ΔE_p) are 49, 49 and 83 mV, respectively, which indicates

that three of them are the single-electron processes^[25]. It can be considered that the redox couples were attributed to reduction process of Mo^{VI} centers.

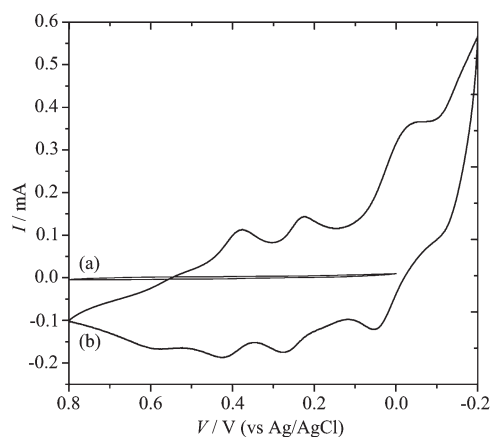


Fig.3 Cyclic voltammograms of (a) the bare CPE and (b) the APM-CPE using the title compound as modifier in 1 mol·L⁻¹ H₂SO₄ at a scan rate of 50 mV·s⁻¹

2.3 Electrocatalytic oxidation of AA at APM-CPE

At bare CPE, the electrooxidation of ascorbic acid requires a large overpotential, and an anodic current was observed at about 480 mV in 1.0 mol·L⁻¹ H₂SO₄. Fig.4a shows the cyclic voltammograms of the bare CPE in 1.0 mol·L⁻¹ H₂SO₄ containing 20 mmol·L⁻¹ AA. No obvious peak is observed in the range 800 mV to -200 mV on the bare electrode in Fig.4a. Fig.4 (b~e) shows the cyclic voltammograms obtained for a series of ascorbic acid solutions with various concentrations. From Fig.4 (b~e), it can be seen that the anodic peak currents obtained increases with increasing ascorbic acid concentration in the solution. The anodic peak

potential (E_{pa}) is about 420 mV (versus standard Ag/AgCl electrode), which is 60 mV lower than that at the bare carbon paste electrode. It seemed that APM-CPE could catalyze oxidation of AA.

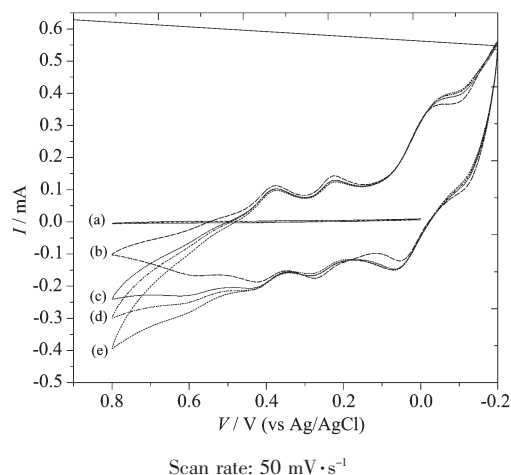


Fig.4 Cyclic voltammograms of a bare CPE in the 20 mmol·L⁻¹ AA+1 mol·L⁻¹ H₂SO₄ solution (a) and a APM-CPE in 1 mol·L⁻¹ H₂SO₄ containing AA with concentrations of 0 (b), 10 (c), 20 (d) and 40 (e) mmol·L⁻¹, respectively

References:

- [1] Fujita M, Kwon Y J, Washiza S, et al. *Am. Chem. Soc.*, **1994**, **116**:1151~1152
- [2] Hagrman P J, Hagrman D, Zubieta J. *Angew. Chem., Int. Ed.*, **1999**, **38**(18): 2638~2684
- [3] Lawandy M A, Huang X, Wang R J, et al. *Inorg. Chem.*, **1999**, **38**(24):5410~5418
- [4] Li H, Eddaoudi M, O'keeffe M, et al. *Nature*, **1999**, **402**:276~279
- [5] Holliday B J, Mirkin C A. *Angew. Chem., Int. Ed.*, **2001**, **40**(11):2022~2043
- [6] Li Y G, Hao N, Wang E B, et al. *Inorg. Chem.*, **2003**, **42**(8): 2729~2735
- [7] Shi Z, Feng S H, Gao S, et al. *Angew. Chem., Int. Ed.*, **2000**, **39**(13):2325~2327
- [8] Shi Z, Li G H, Zhang D, et al. *Inorg. Chem.*, **2003**, **42**(7):2357~2361
- [9] Barthelet K, Riou D, Nogues M, et al. *Inorg. Chem.*, **2003**, **42**(5):1739~1743
- [10] Desiraju G R. *Angew. Chem., Int. Ed. Engl.*, **1995**, **34**(21): 2311~2327
- [11] MacDonald J C, Whitesides G M. *Chem. Rev.*, **1994**, **94**:2383~2420
- [12] Tadokoro M, Isobe K, Uekusa H, et al. *Angew. Chem., Int. Ed.*, **1999**, **38**(1~2):95~98
- [13] Xu Y, An L H, Koh L L. *Chem. Mater.*, **1996**, **8**:814~818
- [14] Zhang Y, Chesfield A, Haushalter R C. *Chem. Commun.*, **1996**:1055~1056
- [15] Li Y G, Wang E B, Zhang H, et al. *Solid State Chem.*, **2002**, **163**:10~16
- [16] Zapf P J, Haushalter R C, Zubieta J. *Chem. Mater.*, **1997**, **9**: 2019~2024
- [17] Hagrman P J, LaDuca Jr R L, Hoo H J, et al. *Inorg. Chem.*, **2000**, **39**(20):4510~4519
- [18] Bi L H, Wang E B, Xu L, et al. *Inorg. Chim. Acta*, **2000**, **305**: 163~167
- [19] Ulrich Kortz. *Inorg. Chem.*, **2000**, **39**(3):623~624
- [20] You W S, Wang E B, Xu Y, et al. *Inorg. Chem.*, **2001**, **40**(21): 5468~5471
- [21] Li L D, Li W J, Sun C Q. *Electroanalysis*, **2002**, **14**(5):368~375
- [22] Neier R, Trojanowski C, Mattes R J. *Chem. Soc. Dalton Trans.*, **1995**:2521~2528
- [23] Peng J, Wang E B, Zhou Y S. *J. Chem. Soc. Dalton Trans.*, **1998**:3865~3869
- [24] Evans H T, Pope M T. *Inorg. Chem.*, **1984**, **23**(4):501~504
- [25] Chen L, Tian X F. *Anal. Bioanal. Chem.*, **2005**, **382**:1187~1195